J Eng Math (2020) 123:165–171
https://doi.org/10.1007/s10665-020-10060-9

Explicit estimates versus numerical bounds for the electrical conductivity of dispersions with dissimilar particle shape and distribution

Ignacio Ochoa · Martín I. Idiart

Received: 20 August 2019 / Accepted: 13 June 2020 / Published online: 1 August 2020

Abstract An effective-medium theory for the electrical conductivity of Ohmic dispersions taking explicit account of particle shape and spatial distribution independently is available from the work of Ponte Castañeda and Willis [J Mech Phys Solids 43:1919–1951, 1996]. When both shape and distribution take particular "ellipsoidal" forms, the theory provides analytically explicit estimates. The purpose of the present work is to evaluate the predictive capabilities of these estimates when dispersions exhibit dissimilar particle shape and distribution. To this end, comparisons are made with numerical bounds for coated ellipsoid assemblages computed via the finite element method. It is found that estimates and bounds exhibit good agreement for the entire range of volume fractions, aspect ratios, and conductivity contrasts considered, including those limiting values corresponding to an isotropic distribution of circular cracks. The fact that the explicit estimates lie systematically within the numerical bounds hints at their possible realizability beyond the class of isotropic dispersions.

Keywords Composites · Conductivity · Finite elements · Homogenization · Porosity

1 Introduction

Unlike some properties of mixtures which follow from simply averaging the properties of the constitutive phases, the electrical conductivity of solid dispersions exhibits an intricate relationship with that of the constitutive phases

I. Ochoa
Facultad de Ingeniería, Universidad de Buenos Aires, Avda. Paseo Colón 850, Ciudad Autónoma de Buenos Aires, C1063ACV Buenos Aires, Argentina

I. Ochoa
Present address: Altran, Limburglaan 24, 5652 AA Eindhoven, The Netherlands
e-mail: onacho87@gmail.com

M. I. Idiart
Departamento de Aeronáutica, Facultad de Ingeniería, Universidad Nacional de La Plata, Avda. 1 esq. 47, B1900TAG La Plata, Argentina

M. I. Idiart
Consejo Nacional de Investigaciones Científicas y Técnicas (CONICET), CCT La Plata, Calle 8 N° 1467, B1904CMC La Plata, Argentina
e-mail: martin.idiart@ing.unlp.edu.ar

[1]. Several multi-scale theories have been proposed to quantify such relationship. A particularly rigorous effective-medium theory for Ohmic dispersions taking explicit account of particle shape and spatial distribution independently is available from the work of Ponte Castañeda and Willis [2]. When both shape and distribution take particular "ellipsoidal" forms, the theory provides analytically explicit estimates. These estimates were initially proposed in the context of linearly elastic composites, and have been hitherto employed to study the influence of microstructural anisotropy on a wider range of material behaviors including electrical conductivity—see, for instance, the work of Giordano [3] and references therein. However, confidence in their predictive capabilities relies mostly on their ability to recover various exact solutions, none of which exhibits *dissimilar* particle shape and distribution. This is presumably because of a difficulty in identifying dispersions with relevant microstructural statistics whose properties can be exactly determined or narrowly bounded. The present work reports results for one such class of dispersions. The sections that follow recall the explicit estimates and the relevant formulae, describe the special class of dispersions considered along with the numerical methodology to bound their electrical conductivities, and conclude with a presentation and discussion of the relevant results.

2 Explicit estimates for spheroidal dispersions

Ponte Castañeda and Willis [2] considered dispersions with statistically uniform and ergodic microstructures. When the dispersion is composed of a single family of ellipsoidal particles of equal shape and orientation, their estimate for the effective electrical conductivity tensor $\widetilde{\boldsymbol{\sigma}}$ relating the vectors representing macroscopic current density and electric field intensity is given by

$$\widetilde{\boldsymbol{\sigma}} = \boldsymbol{\sigma}^{(1)} + c^{(2)} \left[\left(\boldsymbol{\sigma}^{(2)} - \boldsymbol{\sigma}^{(1)} \right)^{-1} + \left(\mathbf{P}_s - c^{(2)} \mathbf{P}_d \right) \right]^{-1}, \tag{1}$$

where $c^{(r)}$ and $\boldsymbol{\sigma}^{(r)}$ denote the volume fractions and electrical conductivity tensors of the matrix phase ($r = 1$) and the particles ($r = 2$), respectively, while $\mathbf{P}_s$ and $\mathbf{P}_d$ are two microstructural tensors depending on the ellipsoidal symmetry of the particle shape (s) and distribution (d), respectively. The latter are given by the same expression [4]

$$\mathbf{P}_{s,d} = \frac{\det \mathbf{Z}_{s,d}}{4\pi} \int_{|\boldsymbol{\xi}|=1} \frac{\boldsymbol{\xi} \otimes \boldsymbol{\xi}}{\boldsymbol{\xi} \cdot \boldsymbol{\sigma}^{(1)} \boldsymbol{\xi}} |\mathbf{Z}_{s,d} \boldsymbol{\xi}|^{-3} \mathrm{d}\boldsymbol{\xi}, \tag{2}$$

where $\mathbf{Z}_s$ and $\mathbf{Z}_d$ are second-order tensors characterizing the principal directions and semi-axes of the ellipsoidal shape and distribution, respectively, and the integration is defined over the set of unit vectors $\boldsymbol{\xi}$. More precisely, the tensor $\mathbf{Z}_s$ is such that the set of material points $\mathbf{x}$ occupied by a particle centered at $\mathbf{x}_\alpha$ is given by $|\mathbf{Z}_s^{-1}(\mathbf{x} - \mathbf{x}_\alpha)| < 1$, while the tensor $\mathbf{Z}_d$ is such that the joint probability density of finding particles centered at material points $\mathbf{x}$ and $\mathbf{x}'$ depends on those points through the combination $|\mathbf{Z}_d^{-1}(\mathbf{x} - \mathbf{x}')|$. Perfect electric contact is assumed at all internal material interfaces.

When the constitutive phases are isotropic and both particle shape and distribution exhibit colinear spheroidal symmetries, the estimate reduces to

$$\widetilde{\sigma}_{\parallel,\perp} = \sigma^{(1)} + c^{(2)} \left[\left(\sigma^{(2)} - \sigma^{(1)} \right)^{-1} + \left(P_{\parallel,\perp}(w_s) - c^{(2)} P_{\parallel,\perp}(w_d) \right) \sigma^{(1)^{-1}} \right]^{-1}, \tag{3}$$

where $\widetilde{\sigma}_\parallel$ and $\widetilde{\sigma}_\perp$ denote the conductivities of the dispersion along directions parallel and perpendicular to the symmetry axis, $\sigma^{(r)}$ denote the isotropic conductivities of the individual phases, $w_{s,d} = a_\parallel^{s,d} / a_\perp^{s,d}$ are the aspect ratios of the particle shape and distribution, $a_\parallel^s$ and $a_\perp^s$ are the axial and perpendicular semi-axes of the spheroidal shape, $a_\parallel^d$ and $a_\perp^d$ are the axial and perpendicular semi-axes of the spheroidal distribution, and the functions $P_{\parallel,\perp}$ are given by

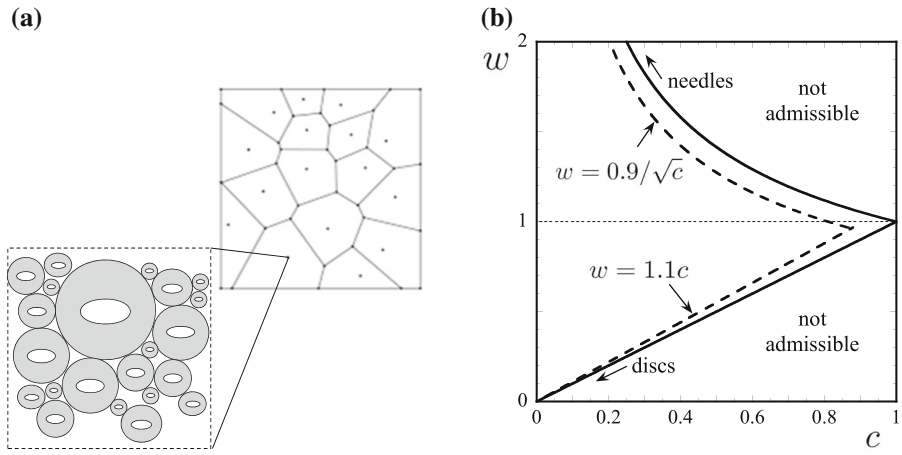

Fig. 1 **a** A Voronoi tessellation filled by composite sphere assemblages. **b** Admissible combinations of particle volume fractions (c) and aspect ratios (w)

$$P_{\parallel}(w) = w\frac{\sinh^{-1}\sqrt{w^2-1}}{(w^2-1)^{3/2}} - \frac{1}{w^2-1} \quad \text{and} \quad P_{\perp}(w) = \frac{1-P_{\parallel}(w)}{2} \tag{4}$$

as shown in the Appendix. Note that these expressions are valid for $w > 1$, but corresponding expressions for $w < 1$ follow by analytic continuation. In the limit of spherical symmetry ($w \to 1$) these expressions give $P_{\parallel}(1) = P_{\perp}(1) = 1/3$. Thus, in the case of isotropic dispersions of spheroidal particles the estimate (3) for the axial conductivity reduces to

$$\widetilde{\sigma}_{\parallel} = \sigma^{(1)} + c^{(2)}\left[\left(\sigma^{(2)} - \sigma^{(1)}\right)^{-1} + \left(P_{\parallel}(w_s) - \frac{c^{(2)}}{3}\right)\sigma^{(1)-1}\right]^{-1}. \tag{5}$$

Henceforth, attention is restricted to this class of spheroidal dispersions.

3 Numerical bounds for a class of spheroidal dispersions

We consider a special class of spheroidal dispersions consisting of non-overlapping homothetic composite spheres of infinite sizes filling up the entire material volume, each composed of an exterior spherical coating made up of the matrix phase and an interior concentric spheroid made up of the inclusion phase; see Fig. 2. These microstructures are variations of the so-called composite sphere and composite ellipsoid assemblages of Hashin [5] and Milton [6]. In particular, we focus on those members of the class where the particle centers are isotropically distributed. That there are indeed members of this type can be easily verified by considering the following construction. Take a Voronoi tessellation of the entire material volume generated by a Poisson random point field, and fill each cell of the tessellation with a composite sphere assemblage that is uncorrelated with the composite sphere assemblages in the other cells, see Fig. 1a. The resulting distribution of particle centers is isotropic regardless of particle shape [7]. When the particles share the spherical symmetry of the coating, the effective conductivity can be determined exactly by solving the field equations within a single composite sphere subject to uniform boundary conditions [5,6]. When the particles are spheroids, by contrast, this procedure no longer provides exact results but it does provide bounds [5,8,9]. In particular, the effective conductivity along the symmetry axis of the spheroidal dispersion is bounded by

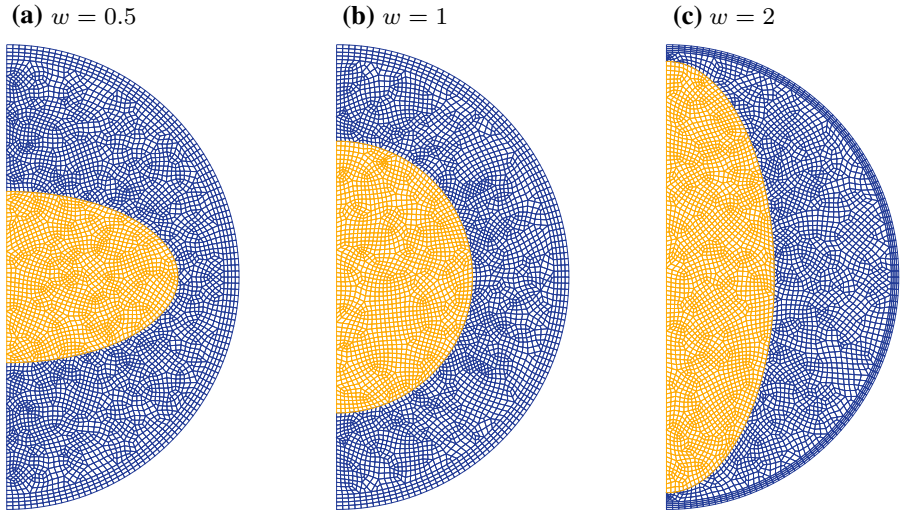

Fig. 2 Discretized domains for a moderate particle volume fraction ($c = 0.2$) and various aspect ratios ($w = 0.5, 1, 2$). (Color figure online)

$$\left[\sum_{r=1}^{2} c^{(r)}(\sigma^{(r)})^{-1}\left(\overline{\overline{J}}^{(r)}/\,\overline{J}\right)^2\right]^{-1} \leq \widetilde{\sigma}_{\parallel} \leq \sum_{r=1}^{2} c^{(r)}\sigma^{(r)}\left(\overline{\overline{E}}^{(r)}/\,\overline{E}\right)^2, \tag{6}$$

where $\overline{\overline{E}}^{(r)} = \sqrt{\langle \mathbf{E}(\mathbf{x})^2\rangle^{(r)}}$ are the second moments of the electric field within each phase r of a composite sphere subject to an electric potential $\overline{E}\,\mathbf{e}\cdot\mathbf{x}$ on its boundary, and $\overline{\overline{J}}^{(r)} = \sqrt{\langle \mathbf{J}(\mathbf{x})^2\rangle^{(r)}}$ are the second moments of the current density field within each phase r of a composite sphere subject to a normal current density $\overline{J}\,\mathbf{e}\cdot\mathbf{n}$ on its boundary. In these expressions, $\mathbf{e}$ and $\mathbf{n}$ are unit vectors denoting the symmetry axis and the outward normal of the composite sphere, respectively. Inequalities (6) follow from well-known variational representations for the effective properties of composites [6]. The electric and current density fields are obtained here by means of the finite element method implemented in a Python code. In view of the axial symmetry of the problem, a cross section of the composite sphere is discretized into quadrilateral isoparametric elements and integrals are evaluated by four-point Gauss quadrature. The meshes are generated by means of the open code Gmsh. Typical meshes are shown in Fig. 2. All elements are forced to lie entirely within a single phase. The method employs the electric potential as the primal variable, which is assumed continuous throughout the domain including internal material interfaces. The limiting case of voided inclusions ($\sigma^{(2)} = 0$) is solved by imposing vanishing normal current directly on the particle–matrix interface. Details of the implementation have been given by Ochoa [10].

4 Results and discussion

In this section, we report comparisons between the explicit estimates (5) and the numerical bounds (6). It is emphasized that the numerical bounds correspond to material systems that belong to the class considered by the explicit estimates, so comparisons are rigorously meaningful. To ease notation, we refer to the volume fraction of particles as $c^{(2)} \equiv c$ and to the particle aspect ratio as $w_s \equiv w$. The fact that the semi-axes of the spheroidal particles must be smaller than the exterior coating radius requires that

$$c \leq w \leq c^{-1/2}. \tag{7}$$

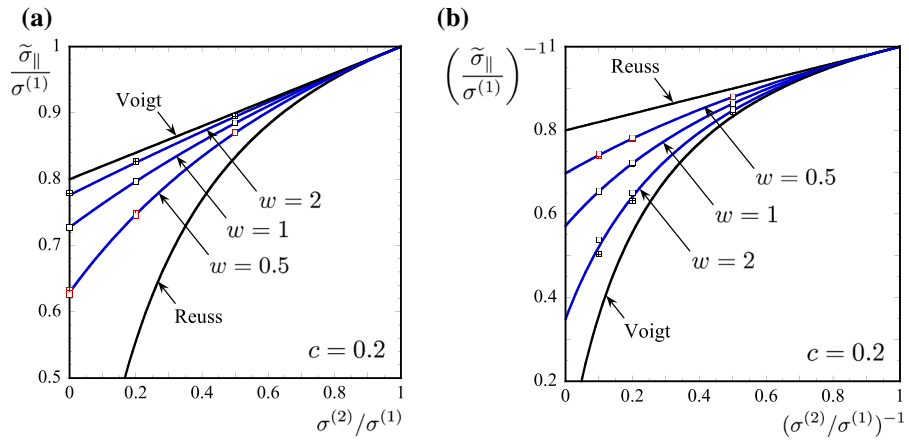

Fig. 3 Effective conductivity versus conductivity contrast, for a moderate volume fraction of particles ($c = 0.2$) and several particle aspect ratios ($w = 0.5, 1, 2$). Continuous lines represent explicit estimates (blue) and elementary bounds (black), while squared symbols represent numerical bounds. (Color figure online)

These two inequalities define a set of admissible microgeometries in the $c - w$ plane as shown in Fig. 1b.

Figure 3 shows comparisons for a moderate volume fraction of particles ($c = 0.2$) and three different aspect ratios ($w = 0.5, 1, 2$) versus conductivity contrast. The explicit estimates (1) are displayed in continuous lines, while the upper and lower bounds (6) are displayed as squared symbols. The elementary bounds of Reuss and Voigt, which are insensitive to particle shape and distribution, are also included for reference. We begin by noting that the estimates and bounds for spherical dispersions ($w = 1$) agree exactly for the entire range of conductivity contrasts, as they should since both procedures are known to deliver the exact solution for composite assemblages of spheres. The main observation in the context of this figure, however, is that the agreement remains good for both oblate ($w = 0.5$) and prolate ($w = 2$) dispersions, even for the strongest conductivity contrasts. Indeed, the numerical upper and lower bounds are found to differ by about 1 % at most when $\sigma^{(2)}/\sigma^{(1)} \ll 1$ and by about 7 % at most when $\sigma^{(2)}/\sigma^{(1)} \gg 1$, thus providing fairly precise values for the exact effective conductivity of the composite assemblages being considered. In turn, the explicit estimates are always found to lie within these bounds, thus providing accurate predictions for the entire range of parameters.

Figure 4 shows similar comparisons for voided inclusions ($\sigma^{(2)} = 0$) and conductive particles ($\sigma^{(2)} = 5\sigma^{(1)}$) versus volume fraction of particles. To guarantee compliance with the requirement (7), the aspect ratio is varied with volume fraction according to $w = 1.1c$ in one case and to $w = 0.9c^{-1/2}$ in another case, see Fig. 1. As the volume fraction tends to zero, these two cases tend to isotropic dispersions of circular discs and straight needles. Once again, good agreement between the numerical bounds and the explicit estimates is observed. The spread between the upper and lower bounds is found to be less than six per cent for all cases except for dispersions of voided inclusions ($\sigma^{(2)} = 0$) with aspect ratios $w = 1.1c$, where the spread exceeds 30 %. This last case is of particular relevance since the limit of vanishing volume fraction ($c \to 0$) corresponds to isotropic distributions of non-conductive circular cracks with ratio of crack radius to spherical coating radius of $1.1^{-1/3} \approx 0.97$. Remarkably, the explicit estimates remain accurate even for this demanding case. This observation, along with the fact that the estimates lie systematically within the numerical bounds—up to numerical accuracy—suggest that the realizability of the estimates for spherical dispersions ($w = 1$) may actually remain valid more general ellipsoidal dispersions.

A completely analogous study has been carried out in the context of fibrous material systems. In this case, the microgeometries are infinitely long parallel fibers with elliptical cross sections isotropically distributed in the transverse plane. The explicit estimates of Sect. 2 for the effective transverse conductivities along the axes of elliptical symmetry are given by the same expression (3) but with the functions (4) replaced by

$$P_{\parallel}(w) = \frac{1}{1+w} \quad \text{and} \quad P_{\perp}(w) = 1 - P_{\parallel}(w). \tag{8}$$

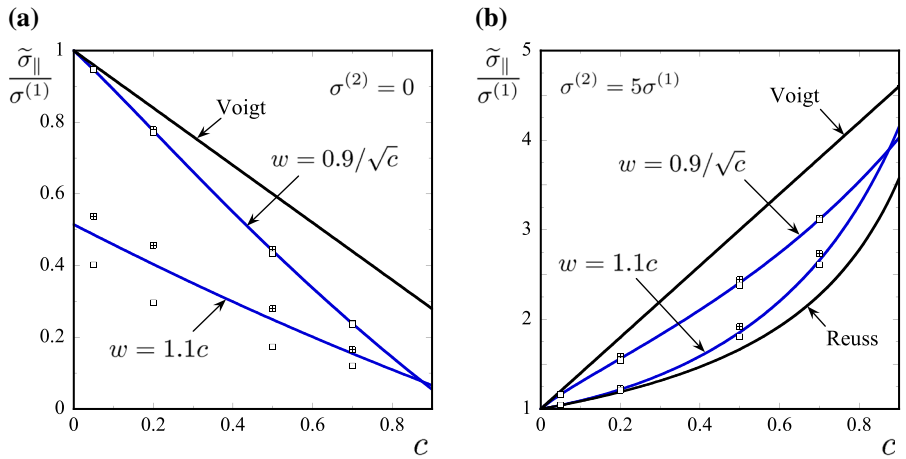

Fig. 4 Effective conductivity versus particle volume fraction for two sequences parametrized by $w = 1.1c$ and $w = 0.9c^{-1/2}$. Continuous lines represent explicit estimates (blue) and elementary bounds (black), while squared symbols represent numerical bounds

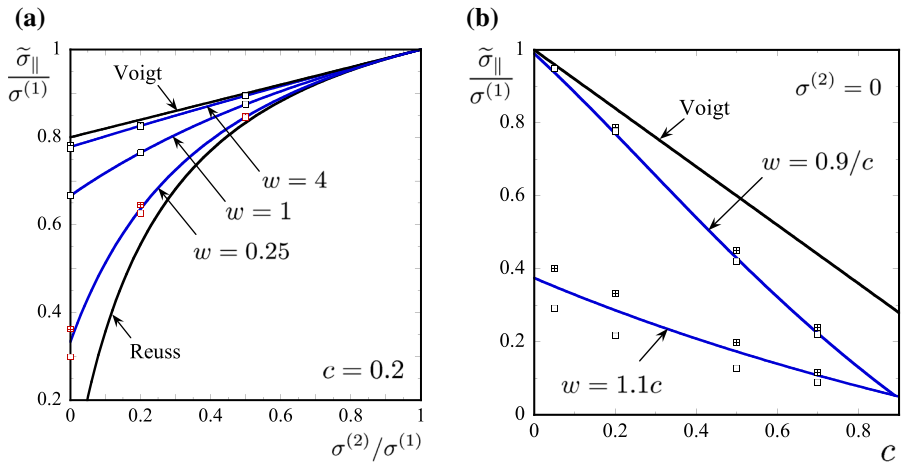

Fig. 5 Effective transverse conductivity versus conductivity contrast, for a moderate volume fraction of fibers ($c = 0.2$) and several fiber aspect ratios ($w = 0.5, 1, 2$). Continuous lines represent explicit estimates (blue) and elementary bounds (black), while squared symbols represent numerical bounds

In turn, numerical bounds for the transverse conductivities can be obtained with the same discretized domains of Sect. 3 but with suitably adapted expressions for the various numerical integrations. The set of admissible volume fractions and aspect ratios of fibers is $c \leq w \leq c^{-1}$. Figure 5 shows results for the transverse effective conductivity along a symmetry axis of the ellipsoidal particles. The good agreement already observed in the context of spheroidal dispersions carries over to this case, even in the limiting case of slit cracks. The above observations for spheroidal dispersions are thus valid for a wider class of material systems.

We conclude by noting that further studies can be carried out for dispersions with more general conduction mechanisms involving, for instance, nonlinear relations between current and electric field or imperfect contacts between matrix and particles. These topics are currently being investigated and will be addressed in a forthcoming publication.

Acknowledgements The work of M.I.I. was funded by the Agencia Nacional de Promoción Científica y Tecnológica through Grant PICT-2014-1988 and by the Universidad Nacional de La Plata through Grant I-2017-225.

Appendix: The tensor P for an isotropic tensor $\sigma^{(1)}$ and an axisymmetric tensor Z

Let $\boldsymbol{\sigma}^{(1)} = \sigma^{(1)}\mathbf{I}$ and $\mathbf{Z} = a_\parallel \mathbf{e}\otimes\mathbf{e} + a_\perp(\mathbf{I} - \mathbf{e}\otimes\mathbf{e})$, where $\mathbf{I}$ is the identity tensor and $\mathbf{e}$ is the unit vector indicating the direction of axial symmetry of $\mathbf{Z}$. In view of the isotropy of $\boldsymbol{\sigma}^{(1)}$, the corresponding tensor $\mathbf{P}$, as given by (2), inherits the axial symmetry of $\mathbf{Z}$. Thus, we can write $\sigma^{(1)}\mathbf{P} = P_\parallel \mathbf{e}\otimes\mathbf{e} + P_\perp(\mathbf{I} - \mathbf{e}\otimes\mathbf{e})$, where

$$P_\parallel = \mathbf{e}\cdot\mathbf{P}\mathbf{e} = \frac{\det\mathbf{Z}}{4\pi}\int_{|\boldsymbol{\xi}|=1}(\mathbf{e}\cdot\boldsymbol{\xi})^2|\mathbf{Z}\boldsymbol{\xi}|^{-3}\mathrm{d}\boldsymbol{\xi} = \frac{a_\parallel a_\perp^2}{4\pi}\int_{|\boldsymbol{\xi}|=1}\frac{(\mathbf{e}\cdot\boldsymbol{\xi})^2}{[a_\parallel^2(\mathbf{e}\cdot\boldsymbol{\xi})^2 + a_\perp^2(1-(\mathbf{e}\cdot\boldsymbol{\xi})^2)]^{3/2}}\mathrm{d}\boldsymbol{\xi}$$

$$= \frac{w}{2}\int_0^\pi \frac{\cos^2\varphi}{[\sin^2\varphi + w^2\cos^2\varphi]^{3/2}}\sin\varphi\,\mathrm{d}\varphi \tag{9}$$

$$P_\parallel + 2P_\perp = \mathrm{tr}\mathbf{P} = \frac{\det\mathbf{Z}}{4\pi}\int_{|\boldsymbol{\xi}|=1}|\mathbf{Z}\boldsymbol{\xi}|^{-3}\mathrm{d}\boldsymbol{\xi} = 1. \tag{10}$$

Expressions (4) follow from these.

References

1. Banisi S, Finch JA, Laplante Ar (1993) Electrical conductivity of dispersions: a review. Minerals Eng 6:369–385
2. Ponte Castañeda P, Willis JR (1996) The effect of spatial distribution on the effective behavior of composite materials and cracked media. J Mech Phys Solids 43:1919–1951
3. Giordano S (2017) Nonlinear effective properties of heterogeneous materials with ellipsoidal microstructure. Mech Mater 105:16–28
4. Willis JR (1977) Bounds and self-consistent estimates for the overall properties of anisotropic composites. J Mech Phys Solids 25:185–202
5. Hashin Z (1962) The elastic moduli of heterogeneous materials. J Appl Mech 29:143–150
6. Milton GW (2002) The theory of composites. Cambridge University Press, Cambridge
7. Milton GW (2019) Private communication
8. Barrett KE, Talbot DRS (1996) Bounds for the effective properties of a nonlinear two-phase composite dielectric. In: Markov KZ (ed) Proceedings on 8th international symposium, continuum models and discrete systems. World Scientific, Singapore, pp 92–99
9. Pastor Y, Ponte Castañeda P (2002) Yield criteria for porous media in plane strain: second-order estimates versus numerical results. Compt Rend Mec 330:741–747
10. Ochoa I (2018) Non-linear electrical conductivity in biphasic materials. Masters Thesis, Universidad de Buenos Aires